Research Article

Sana J. Yaseen*

Numerical study of the fluid flow and heat transfer in a finned heat sink using Ansys Icepak

https://doi.org/10.1515/eng-2022-0440
received December 26, 2022; accepted April 07, 2023

Abstract: This research studies a three-dimensional fluid flow, and heat transfer in the heat sink numerically using air as a coolant. The numerical effects of the number of fins and their thickness on the performance of the heat sink are investigated using Ansys Icepak. Various fin numbers and fin thicknesses are used to check the heat sink's optimal thermal performance. The results demonstrated that the maximum temperature, pressure drop, and thermal resistance decrease with the increase in the fin number and thickness. According to the results, the optimal thickness and number of fins for the current study are 15 and 0.25 mm, respectively. Also, it is observed that increasing the number of fins has a greater effect than increasing the thickness of the fins on the maximum temperature, pressure drop, and thermal resistance.

Keywords: ANSYS Icepak, maximum temperature, thermal resistance, heat sink, rectangular fins

1 Introduction

Heat is produced by all electronic devices when they are in use [1]. Almost all industrial applications require temperature reduction, which is essential [2]. The device may fail if exposed to temperatures beyond the safe operating range. Most devices are not certified to work between 50 and 80°C. Each 10°C rise in temperature reduces the component life by 50% [3]. As electronic devices improve, cooling has become one of the most challenging and significant issues to address [4]. Electronic cooling helps reduce the heat rate of electronic equipment and extend the product life [3,5]. Heat sinks promote the spread of heat from their source to the environment by extending their surfaces (fins) [1]. Therefore, heat sinks are used to keep the electronic equipment's temperature below the desired level [6]. To improve convective heat transfer from the heat sinks, the extended surface (fins) is used in various electrical and engineering applications [7].

In this study, the number of fins are varied to find the optimal number that gives the best cooling performance. Therefore, a heat sink without fins and with different numbers of fins and thickness were analyzed in Ansys Icepak.

2 Background study

Escher et al. [8] investigated a three-dimensional model of a very thin electronic heat sink. A 2×2 cm^2 chip with a total thermal resistance of 0.087 cm/W was used to optimize the design. For a 65 K temperature difference between the chip temperature and the fluid inlet temperature, the maximum cooling capacity was 750 W/cm^2.

The heat transport through the heat sink was examined by Kepekci and Asma numerically using computational fluid dynamic CFD software [4]. Straight, square, hexagonal, and airfoil fin shapes were also used in the investigation. They assumed that the CPU and atmosphere would be at 25 and 80°C, respectively, and that air would travel at 7.5 m/s. Each fin was measured at 0.02 m in length and 0.002 m in thickness. They concluded that fins made of silver airfoil provided the optimum cooling performance and cost.

Castelan et al. [9] analyzed heat sinks and fans analytically. During the study, they took a sink with 17 fins with thickness and height of 6.1 and 40 mm, respectively, with the chip length changing throughout. According to their results, the thermal resistance decreased by 12% when heat sink + fan optimization was based on thermal resistance.

Bondareva et al. [10] used the finite difference approach to quantitatively investigate the phase change material performance. The fins utilized were 0.33 cm wide and 5 cm tall. The effects of heat flux and fin size on the phase change material and capacitance were investigated. With a heat load of 1,600 W/m^2, they discovered that the presence of

* **Corresponding author: Sana J. Yaseen,** Mechanical Engineering Department, Basrah University, Basrah, Iraq,
e-mail: sana.yaseen@uobasrah.edu.iq

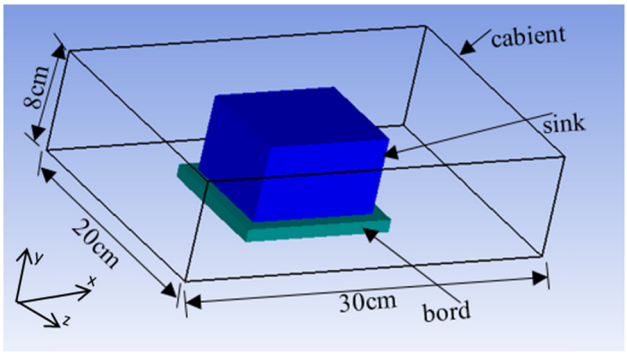

Figure 1: 3D computational domain for the geometry.

transverse ribs could have decreased the source temperature by more than 1,200°C.

Silva et al. [11] numerically studied the heat sink performance using forced convection heat transfer. They discovered that a staggered preparation of pin fins with diameters of 1.5 mm and spacing of 5 mm produced the best case for pin heat sinks. Additionally, they noticed improved thermal performance due to the incorporation of holes into circular pins. They also used three types of heat sinks to show the best sink performance under the same boundary conditions, and they proved that a heat sink with a hexagon shape has the best results.

A study of water as coolant fluid for laminar forced convection in heat sinks with micro-pin fin in a heat sink has been studied numerically by Shafeie et al. [12]. Both pin fin heat sinks and pin-finned microchannel heat sinks (MCHS) were examined using the oblique or staggered distribution of the pin fins. A lower heat removal was achieved for the same pumping powers of 0.5 and 2 W compared with the best simple MCHS. Also, it can be shown that the heat sink with (500 mm) height depth has the maximum heat subtraction.

3 Problem description

In the present study, a rectangular cabinet contains one heat source and a heat sink for the investigation. The upper and the side walls of the cabinet are adiabatic. The heat sink and fins are made of aluminum with a density of 2,800 kg/m^3, and the thermal conductivity is 205 W/m °C. Air is the working fluid, which flows along the x-axis, as shown in Figure 1. The dimensions of the cabinet and its components are given in Table 1.

Table 1: Dimensions of the cabinet components in cm

Component	Height (y)	Length (z)	Width (x)
Cabinet	30	20	8
Board	12	10	1
Heat sink	10	8	6

4 Governing equations

The problem under consideration concerns the flow through the heat sink and the cabinet. Heat transfer in the heat sink unit is a conjugate process, which combines the conduction heat transfer in the solid parts and convection heat transfer through the fluid.

To investigate, the following assumptions are prepared for the model to simplify the momentum and energy equations:

(1) The 3D flow is assumed to be steady-state, incompressible, and laminar.
(2) There will be no slip flow close to the walls.
(3) The energy dissipation is negligible.
(4) The radiation is negligible.
(5) The effect of gravity is negligible.
(6) The liquid and solid assumed has constant properties.

After applying the set of assumptions, the 3D equation system that governs the single-phase model includes the continuity, momentum, and energy equations can be summed up as follows [13]:

$$\frac{\partial u}{\partial x} + \frac{\partial v}{\partial y} + \frac{\partial w}{\partial z} = 0. \tag{1}$$

Momentum in x, y, and z directions, respectively, are:

$$u\frac{\partial u}{\partial x} + v\frac{\partial u}{\partial y} + w\frac{\partial u}{\partial z} = -\frac{1}{\rho}\frac{\partial P}{\partial x} + \frac{\mu}{\rho}\left(\frac{\partial^2 u}{\partial x^2} + \frac{\partial^2 u}{\partial y^2} + \frac{\partial^2 u}{\partial z^2}\right), \tag{2}$$

$$u\frac{\partial v}{\partial x} + v\frac{\partial v}{\partial y} + w\frac{\partial v}{\partial z} = -\frac{1}{\rho}\frac{\partial P}{\partial y} + \frac{\mu}{\rho}\left(\frac{\partial^2 v}{\partial x^2} + \frac{\partial^2 v}{\partial y^2} + \frac{\partial^2 v}{\partial z^2}\right), \tag{3}$$

$$u\frac{\partial w}{\partial x} + v\frac{\partial w}{\partial y} + w\frac{\partial w}{\partial z} = -\frac{1}{\rho}\frac{\partial P}{\partial z} + \frac{\mu}{\rho}\left(\frac{\partial^2 w}{\partial x^2} + \frac{\partial^2 w}{\partial y^2} + \frac{\partial^2 w}{\partial z^2}\right). \tag{4}$$

Energy equation is given as follows:

$$u\frac{\partial T}{\partial x} + v\frac{\partial T}{\partial y} + w\frac{\partial T}{\partial z} = \frac{k}{\rho C_p}\frac{\partial^2 T}{\partial x^2} + \frac{\partial^2 T}{\partial y^2} + \frac{\partial^2 T}{\partial z^2}, \tag{5}$$

where the variables "T" and "P" represent the fluid's temperature and pressure, u, v, and w represent the

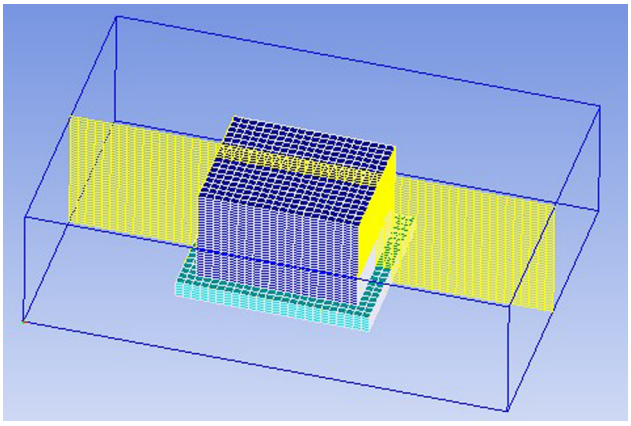

Figure 2: 3D Meshed model with heat sink.

Table 2: Number of nodes, elements, and maximum block temperature

No.	Elements no.	Nodes no.	Temperature of block (K)
1.	8,820	10,164	103.459
2.	31,200	34,317	103.462
3.	96,000	102,591	103.469
4.	160,800	170,865	103.469

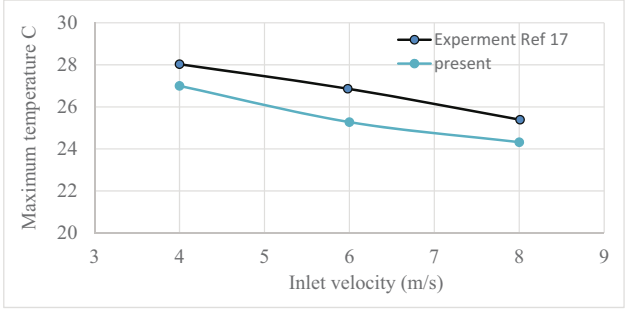

Figure 3: Comparison of the numerical results of the present study with that reported by Adhikari et al. [17].

components of fluid velocity in x, y, and z directions and ρ, μ, and k represent the density, viscosity, and thermal conductivity, respectively.

The energy equation for the solid walls is given as follows [14,15]:

$$\frac{\partial^2 T_s}{\partial x^2} + \frac{\partial^2 T_s}{\partial y^2} + \frac{\partial^2 T_s}{\partial z^2} = 0. \quad (6)$$

It is possible to calculate the heat sink's thermal resistance to know how well it works. To compute the thermal resistance, we must determine the temperature difference and the highest temperature rises in the heat sink. The maximum difference temperature can be calculated as [16]:

$$\Delta T_{max} = T_{s,o} - T_{in}, \quad (7)$$

where $T_{s,0}$ is the heat source's highest temperature, T_{in} is the fluid's temperature at the inlet, equal to 20°C.

Both can be used in the following formulas to calculate the thermal resistance:

$$R_{th} = \Delta T_{max}/Q \quad (°C/W), \quad (8)$$

where Q is the power supplied, which is equal to 50 W.

Table 3: Ranges of parameter values that are studied

Parameter	Value
Fin count	0, 5, 10, 15, and 20
Fin thickness	0.05, 0.1, 0.15, 0.2, and 0.25 mm

4.1 Boundary conditions (BCs)

1. BC for the hydrodynamic: uniform velocity at the channel inlet. The no-slip condition was used for all the walls, $u = 0$, $v = 0$, and $w = 0$.
2. All solid region boundaries are subjected to all external walls except for the bottom wall of the heat sink, where constant heat flux is applied. q'' = constant.

The temperature at the inlet is $T = T_{in}$, $-k_s \frac{\partial T_s}{\partial y} = -k_f \frac{\partial T_f}{\partial y}$ at the fluid–solid interface and $T_f = T_s$, $\frac{\partial T}{\partial y} = 0$ at the outlet.

5 Check grid independence

The Ansys Icepak uses a Fluent solver, and the preprocessing generates a Hexa-dominant mesh. The simulation-specific mesh profile is shown in Figure 2.

We investigate how grid refinement affects the numerical solutions for the heat sink without fins. The grid dependence test is first conducted using several different elements and nods. The results obtained from these meshes are summarized in Table 2.

From Table 2, it is clear that with the increase in the number of nodes, the temperature change is very small, especially after case 3. Therefore, the type of mesh chosen for our calculations is the third type.

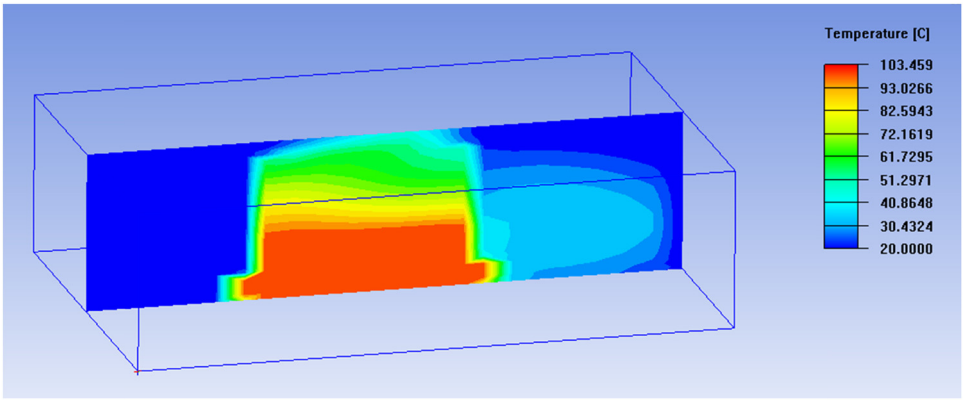

Figure 4: Temperature distribution on a plane in z direction passing through the heat sink, for n = 0.

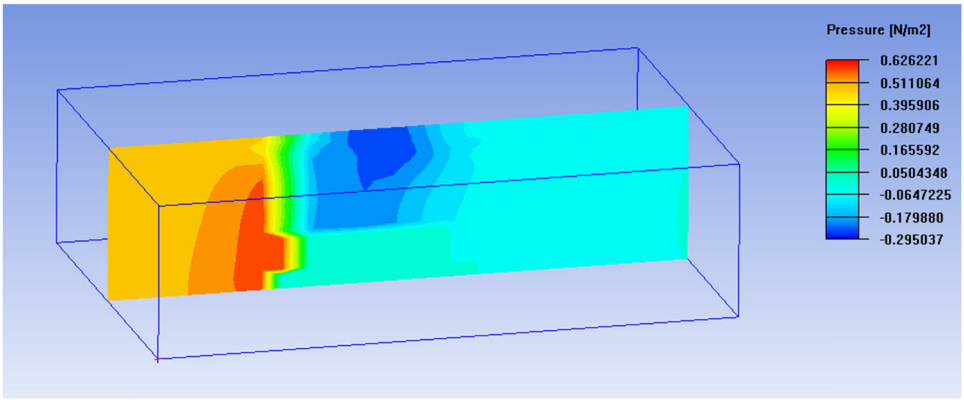

Figure 5: Pressure distribution on a plane in z direction passing through the heat sink, for n = 0.

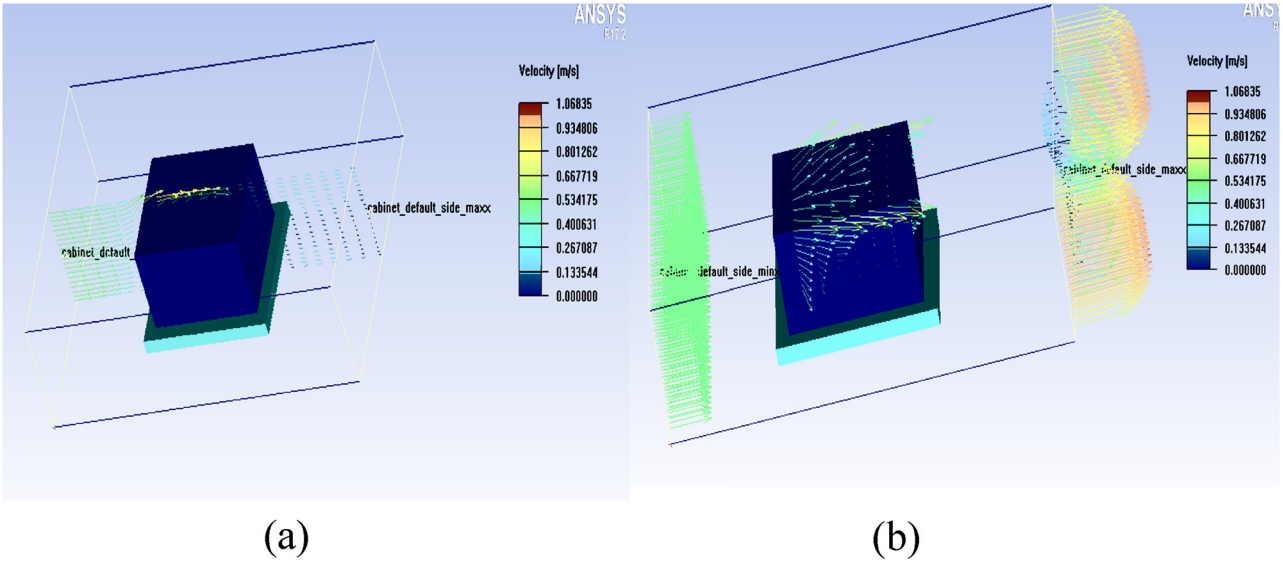

Figure 6: Velocity distribution on (a) heat sink and a plane in the z direction, (b) the cabinet, inlet, and outlet, for n = 0.

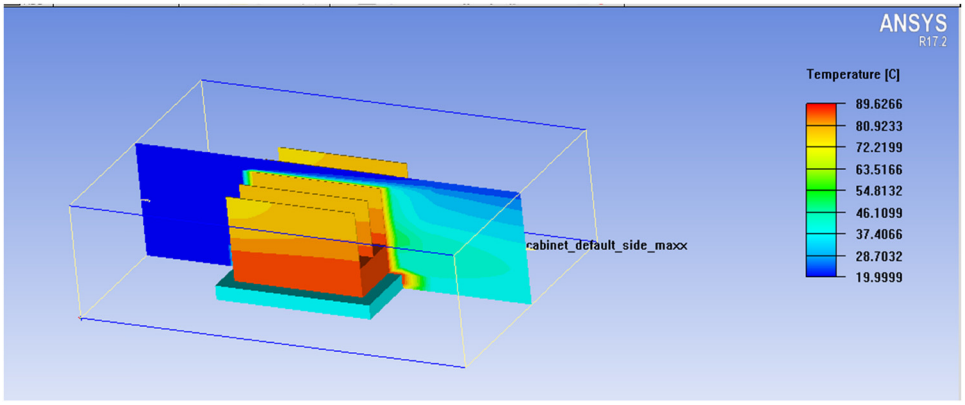

Figure 7: Temperature distribution on a plane in z direction across the heat sink, for n = 5.

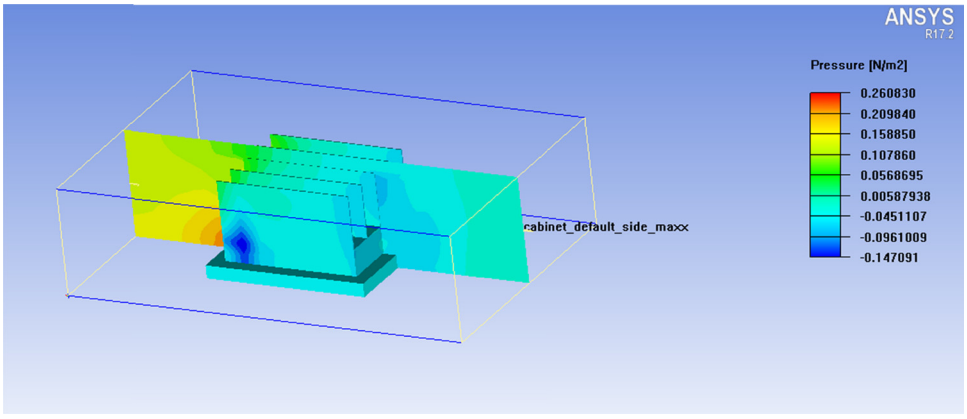

Figure 8: Pressure distribution on a plane in z direction across the heat sink, for n = 5.

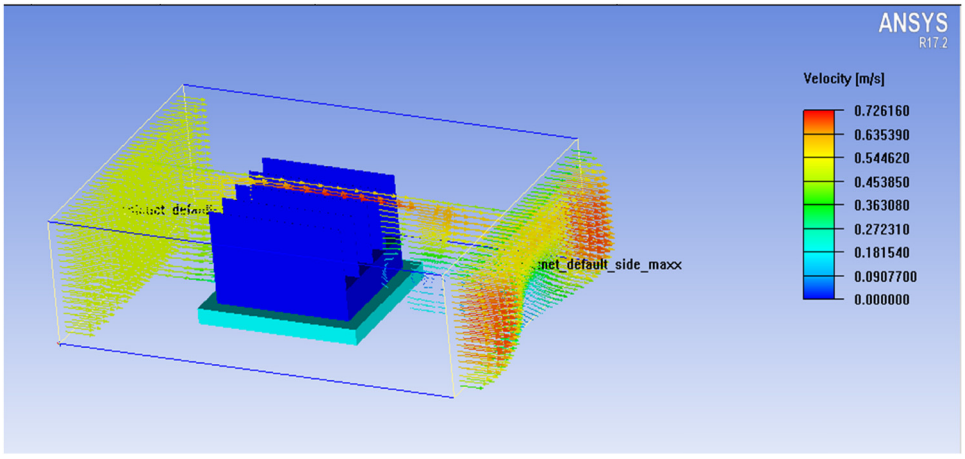

Figure 9: Velocity distribution on a plane in z direction across the heat sink, for n = 5.

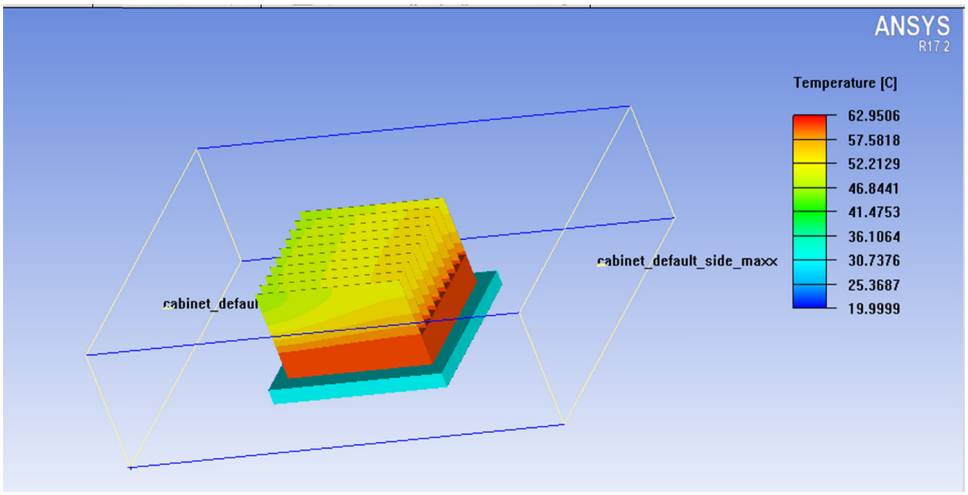

Figure 10: Temperature distribution through the heat sink, for n = 10.

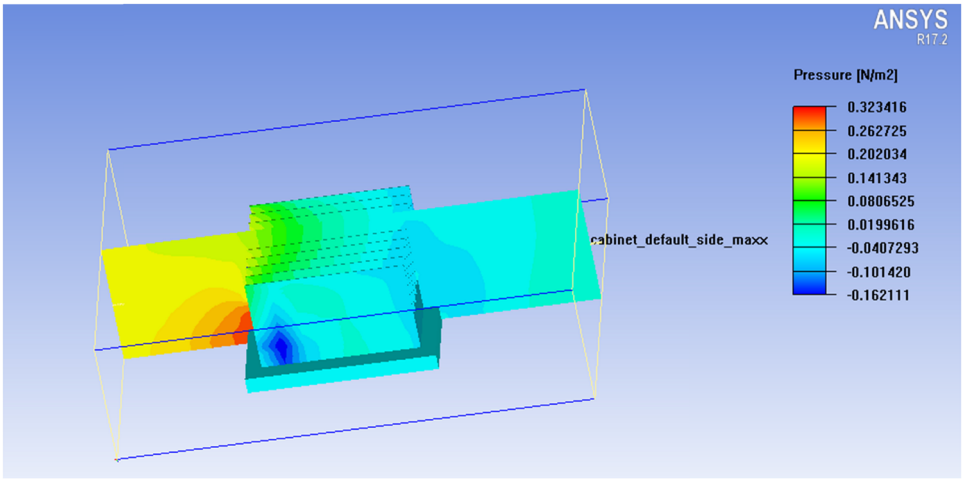

Figure 11: Pressure distribution on a plane in z direction across the heat sink, for n = 10.

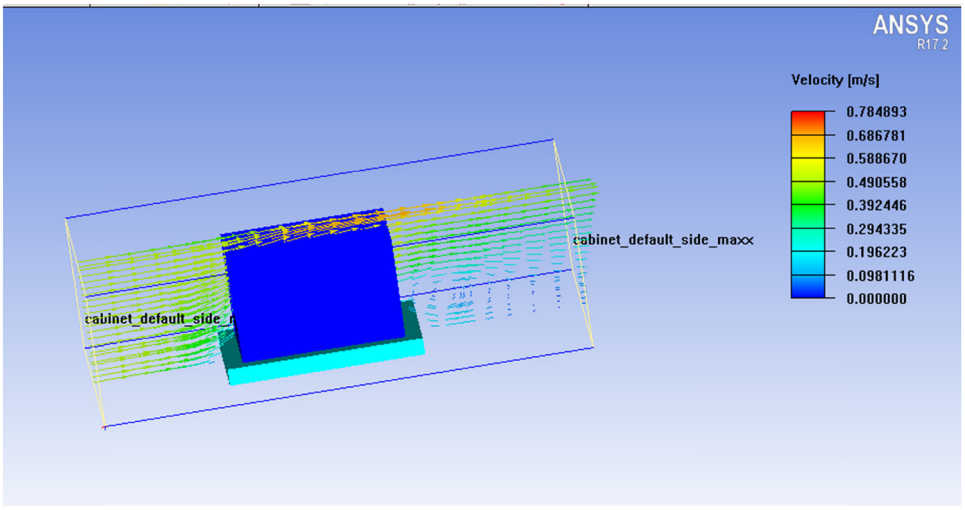

Figure 12: Velocity distribution on a plane in z direction across the heat sink, for n = 10.

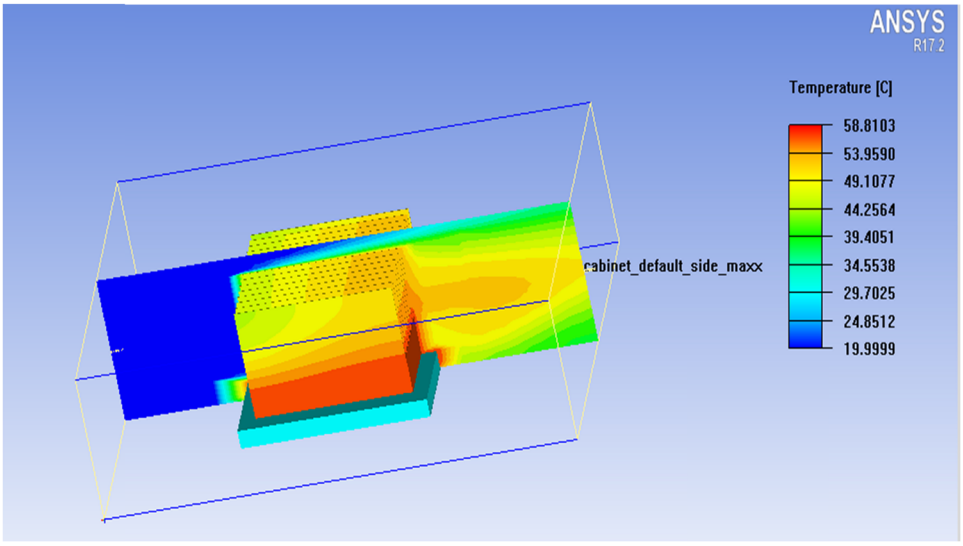

Figure 13: Temperature distribution on a plane in z direction across the heat sink, for n = 15.

6 Numerical method and validation

In the present study, a finite volume method is used to resolve continuity, momentum, and energy equations. The simple algorithm is used to resolve the velocity–pressure coupling, while the equations are discretized using a second-order upwind scheme.

The results of the present study are compared with the experimental data of Adhikari et al. [17] in order to validate our numerical work. They investigated the forced convection heat transfer from a rectangular array of straight fins with incoming flow parallel to fin channels at low Re. The maximum temperatures of the current work and experiment results of the reference [17] for three different velocities 2, 4, and 6 m/s are shown in Figure 3. Figure 3 demonstrates that the current numerical work has a deviation of less than 4.2% from the reference experiment results [17].

7 Results and discussion

The results of hydrodynamic parameters (velocity and pressure) and the thermal characteristic represented by the temperature and thermal resistance distribution in

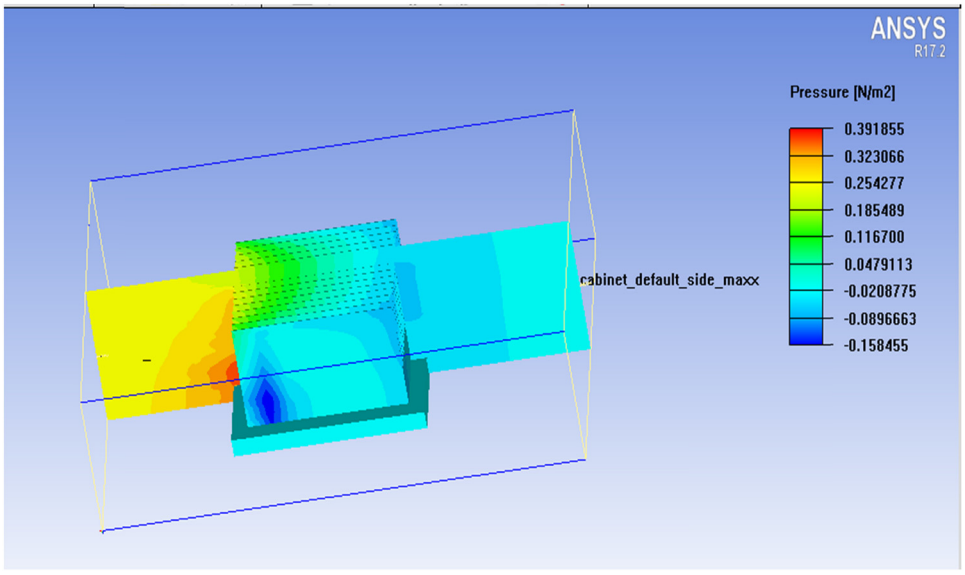

Figure 14: Pressure distribution on a plane in z direction across the heat sink, for n = 15.

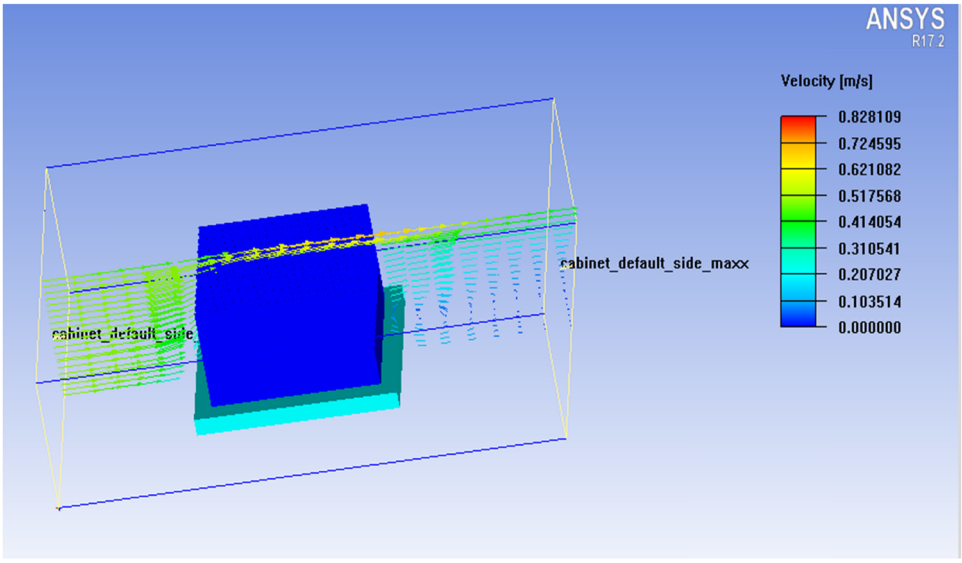

Figure 15: Velocity distribution on a plane in z direction across the heat sink, for n = 15.

the cabinet and the heat sink will be presented. The heat sink's performance is examined concerning the number and thickness of fins. Table 3 shows the range of values for the number and thickness of the fins used in this study.

At first, we run the program for the heat sink without fins. The results of temperature, pressure, and velocity obtained are as shown in Figures 4–6, respectively.

Figure 4 shows that the maximum temperature is 103.459°C when no fin exists. The heat sink has the highest temperature because it is close to the heat source. As we go up to the top, the maximum temperature drops slightly. Figure 5 represents the pressure through the plane in the *yz* direction, and it can be seen that the larger value of pressure is located near the inlet region and reduces along the cabinet until it reaches zero at the outlet because of the reduced velocity from the inlet to outlet as displayed in Figure 6.

The results of temperature, pressure, and velocity distribution along the heat sink, when five fins were added, are shown in Figures 7–9. It can be seen that the maximum temperature is observed in the lower part of the heat sink, which reached 89.626°C, and we note the highest speed reached by the fluid during its crossing through the heat sink is 0.726 m/s. As for the pressure, it was concentrated at the beginning of the cabinet and decreased when passing through the heat sink, where the highest pressure that can be achieved is 0.2608 N/m^2 near the first edge of the heat sink that is directly above the board.

Figures 10–18 show the temperature, pressure, and velocity contours for the cases of fin numbers 10, 15, and 20, respectively. From Figures 10, 13, and 16, the maximum temperature can be seen at the bottom of the heat sink, close to the heat source where the heat flux is applied. This value gradually reduces from the base to the sink top since it

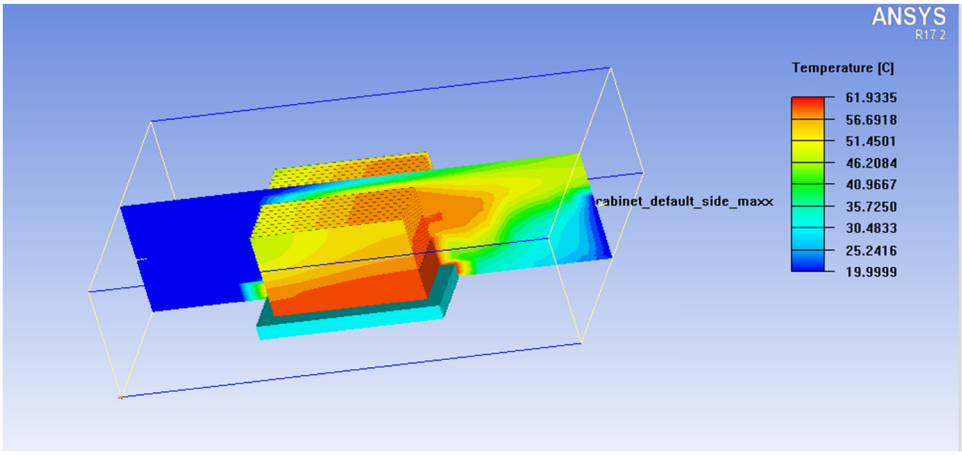

Figure 16: Temperature distribution on a plane in z direction across the heat sink, for n = 20.

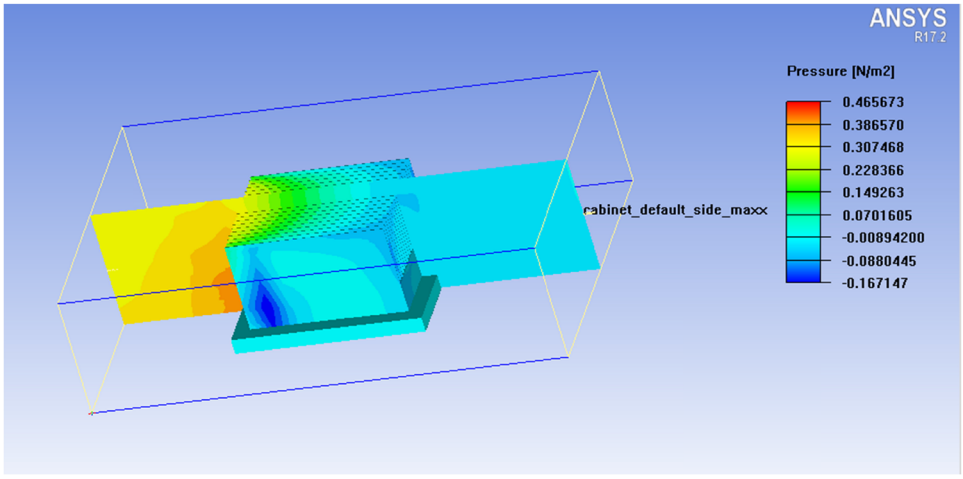

Figure 17: Pressure distribution on a plane in *z* direction across the heat sink, for $n = 20$.

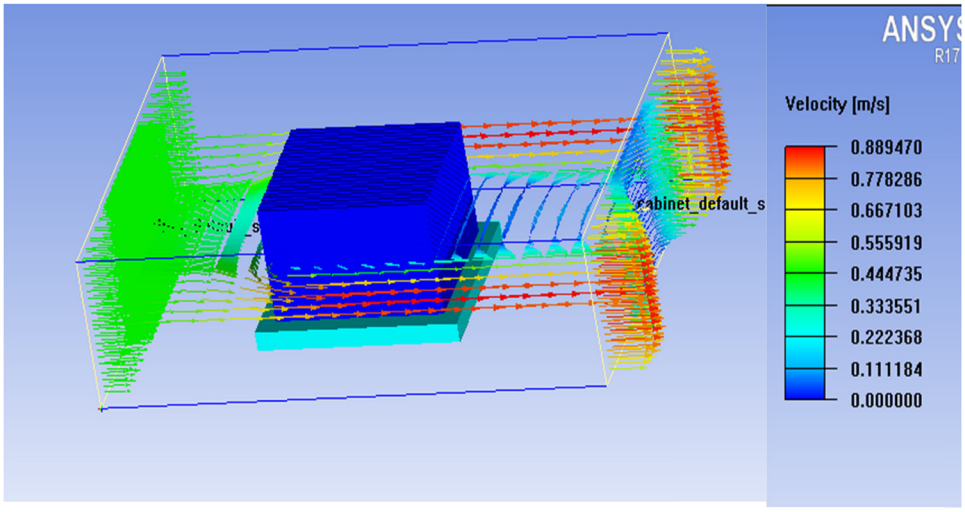

Figure 18: Distribution of velocity on a plane in *y* direction across the heat sink, for $n = 20$.

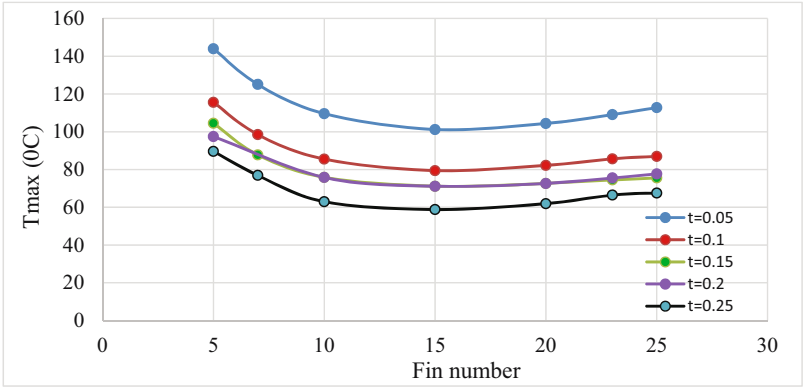

Figure 19: Maximum temperature vs fin numbers at different fin thicknesses.

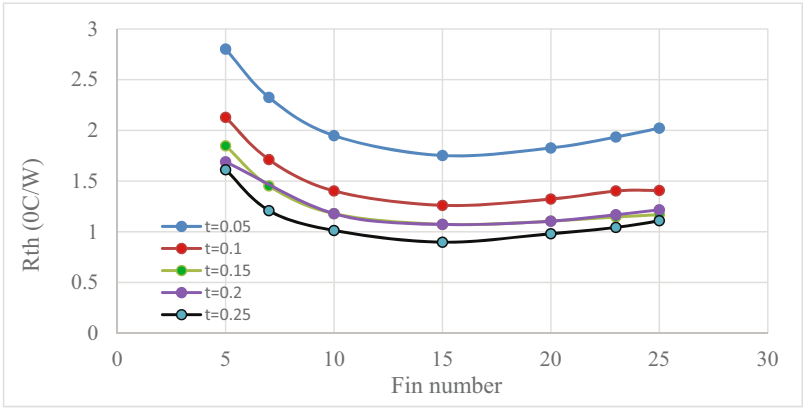

Figure 20: Thermal resistance variation with fin numbers at different fin thicknesses.

is far from the heat source. The optimum pressure and velocity values are located at the inlet area, which decreases gradually until it reaches the exit area of the cabinet, as can be observed in Figures 11, 12, 14, 15, 17, and 18.

Figure 19 draws for maximum temperature vs fin number for different fin thicknesses (t = 0.05, 0.1, 0.15, 0.2, and 0.25). This figure shows that the temperature reduces until it reaches the lowest value at n = 15, then increases again. This is because having more fins with the same thickness shortens the distance between them, which raises the temperature around the fins. Additionally, this prevents air from reaching all of the cooling fins, resulting in low heat transfer rates from the heat source to the moving fluid and an increase in temperature. The addition of more fins works as an obstacle to heat transfer. Therefore, an optimal number of fins gives the lowest maximum temperature for each specific fin thickness. Also, we note from the figure that the best fin thickness gives the lowest maximum temperature t = 0.25 mm, which means that as the thickness increases, the maximum temperature reduces.

The thermal resistance vs fin number for various fin thicknesses is depicted in Figure 20. It can be seen from this illustration that the thermal resistance reduces till it reaches the lowest value at n = 15, then it increases again. The figure shows that the best number of fins that gives the lower thermal resistance value is n = 15, and the best thickness is t = 0.25 mm.

Figure 21 indicates the pressure drop change vs the number of fins at different thicknesses. It can be shown from the figure that the pressure drop through the sink reduces with the increase in the fin thickness. Also, it increases as the fin number increases, and the lowest pressure drop value occurs at t = 0.25 mm.

Figures 19–21 indicate that the optimal number of fins for the current study is 15, and the best thickness is t = 0.25 mm.

8 Conclusion

The optimal thermal performance of the heat sink with various fin thicknesses and numbers is the subject of this

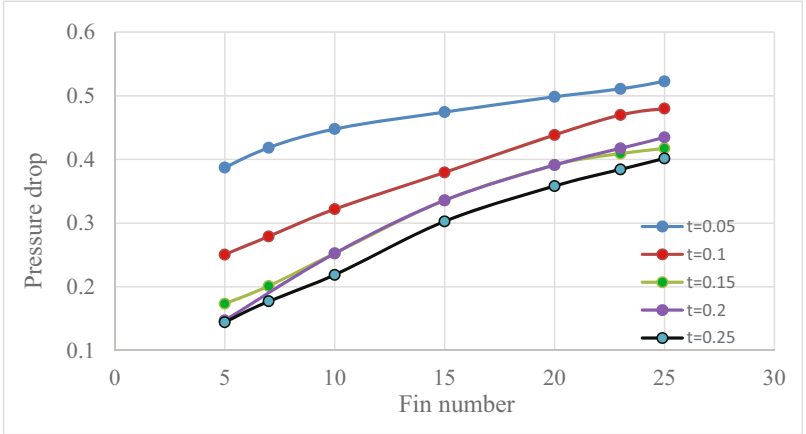

Figure 21: Pressure drop variation with fin numbers at different fin thicknesses.

investigation. The effect of number and thickness of fins on the maximum temperature, pressure drop, and thermal resistance are analyzed numerically using ANSYS ICEPAK.

The following conclusions can be drawn from the findings:

1. The maximum temperature with fins is less than the maximum temperature without fins.
2. The maximum temperature and thermal resistance decrease as the number of fins increases until n = 15; after that, the temperature rises again, so the optimal number of fins is 15.
3. The heat sink has the lowest temperature, pressure drop, and thermal resistance when its fin thickness is 0.25 mm.
4. The decrease in maximum temperature, pressure drop, and thermal resistance is 75.92, 59.775, and 75%, respectively, when 15 fins are used compared to a heat sink without fins.
5. The reduction in the maximum temperature, pressure drop, and thermal resistance is 42, 36.2, and 48.8%, respectively, when 0.25 mm is used compared with 0.05 mm fin thickness for the number of fins equal to 15.
6. It is evident that increasing the number of fins has a significantly greater impact on the maximum temperature, pressure drop, and thermal resistance than increasing the thickness of the fins.

Nomenclature

C_p	constant pressure specific heat
g	acceleration
p	pressure
k	thermal conductivity
q''	heat flux (W/m^2)
Q	power (W)
R_{th}	thermal resistance
T	temperature
u, v, w	Cartesian velocity components
x, y, z	Cartesian co-ordinates
n	number of fins
t	fin thickness

Greek symbols

ρ	density
μ	dynamic viscosity

Subscript

s	solid
f	fluid
max	maximum
o	out
i	in the inlet

Conflict of interest: The authors state no conflict of interest.

Data availability statement: Most datasets generated and analyzed in this study have been provided in this submitted manuscript. The other datasets are available on reasonable request from the corresponding author with the attached information.

References

[1] Dede EM, Josh SN, Zhou F. Topology optimization, additive layer manufacturing, and experimental testing of an air-cooled heat sink. Mech Des Trans ASME. 2015;137:11.

[2] Choong JY, Yu KH, Abdullah MZ. Numerical study of heat transfer characteristics of laminar nanofluids flow in oblique finned microchannel heat sink. J Adv Res Fluid Mech Therm Sci. 2020;76(3):25–37.

[3] Raja B, Praveenkumar V, Leelaprasad M, Manigandan P. Thermal Simulations of an Electronic System using Ansys Icepak. J Eng Res Appl. 2015;5(11):57–68. www.ijera.com.

[4] Kepekci H, Asma A. Comparative analysis of heat sink performance using different materials. Am J Eng Res (AJER). 2020;9(4):204–21. www.ajer.org.

[5] Nazzal IT, Salem TK, Al Doury RR. Theoretical investigation of a pin fin heat sink performance for electronic cooling using different alloys materials. IOP Conference Series: Materials Science and Engineering, INTCSET. 2021.

[6] Kumar Y, Saxena NV. Optimization of heat transfer process parameters for heat sink using CFD. Int J Trend Sci Res Dev (IJTSRD). 2020;4(6):184–7.

[7] Dhumne AB, Farkade HS. Heat transfer analysis of cylindrical perforated fins in staggered arrangement. Int J Innov Technol Explor Eng. 2013;2(5):225–30.

[8] Escher W, Michel B, Poulikakos D. A novel high performance, ultrathin heat sink for electronics. Int J Heat Fluid Flow. 2010;31:586–98.

[9] Castelan A, Cougo B, Dutour S, Meynard T. Analytical modelling of sink heat distribution for fast optimisation of power converters. Electricmacs 2017, Toulouse, France; 2017. p. 296–307.

[10] Bondareva NS, Ghalambaz M, Mikhail A. Influence of the fin shape on heat transport in phase change material heat sink with constant heat loads. Energies. 2021 March 3;14:1389.

[11] Silva EC, Sampaio AM, Pontes AJ. Evaluation of active heat sinks design under forced convection effect of geometric and boundary parameters. Materials. 2021;14(8):2041.
[12] Shafeie H, Abouali O, Jafarpur K, Ahmadi G. Numerical study of heat transfer performance of single-phase heat sinks with micro pin-fin structures. Appl Therm Eng. 2013;58:68–76.
[13] Mohammed AA, Razuqi SA. Performance of rectangular pin-fin heat sink subject to an impinging air flow. J Ther Eng. 2021 Mar;7(No 3):666–76. Istanbul, Turkey: Yildiz Technical University Press.
[14] Patil NG, Hotta TK. Role of working fluids on the cooling of discrete heated modules: a numerical approach Sådhanå. Indian Acad Sci. 2018;43:187.
[15] Yaseen SJ, Rageb AA, Alshara AK. Performance characteristics of Micro-channel heat sink with variable cross-section. Proceedings of the 2nd International Conference Southern Technical University. 2017. p. 102–9.
[16] Shkarah AJ, Sulaima MY, Ayob MR, Togun H. A 3D numerical study of heat transfer in a single-phase micro-channel heat sink using graphene, aluminum and silicon as substrates. Int Commun Heat Mass Transf. 2013;48:108–15.
[17] Adhikari RC, Wood DH, Pahlevani M. An experimental and numerical study of forced convection heat transfer from rectangular fins at low Reynolds numbers. Int J Heat Mass Transf. 2020;63:120418.